JOC Article
pubs.acs.org/joc

Carboxyl BODIPY Dyes from Bicarboxylic Anhydrides: One-Pot Preparation, Spectral Properties, Photostability, and Biolabeling

Dongchuan Wang, Jiangli Fan, Xinqin Gao, Bingshuai Wang, Shiguo Sun, and Xiaojun Peng*

State Key Laboratory of Fine Chemicals, Dalian University of Technology, 158 Zhongshan Road, Dalian 116012, P. R. China

pengxj@dlut.edu.cn

Received June 8, 2009

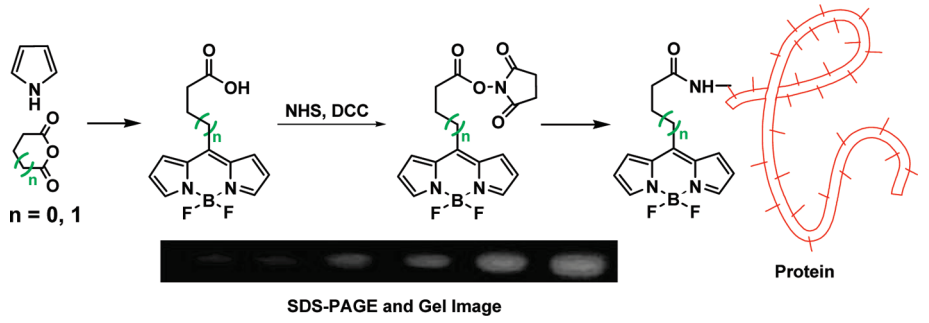

New fluorescent dyes based on 4,4-difluoro-4-bora-3a,4a-diaza-*s*-indacene (BODIPY) and functionalized with a free carboxyl group have been conveniently synthesized from pyrroles and dicarboxylic anhydrides in one-pot reactions. Their spectral properties in different solvents showed little effect of solvatochromism (< 10 nm). The methyl groups on the BODIPY skeleton benefit the fluorescence quantum yields (Φ_f up to 0.80 in water) but affect the photostability of the dyes. Photooxidation and photodegradation experiments suggest that dyes **1a** and **2a** exhibit excellent photostability, especially in water, and several factors were taken into account to elucidate the experimental phenomena. Dyes **1c** and **2c**, derived from **1a** and **2a** via the esterification of NHS (*N*-hydroxysuccinimidyl ester), can be easily acquired in high yields (> 90%). Single crystal X-ray structures of dyes **2c** and **3a** are also obtained and discussed. The fluorescence labeling of BSA and followed prestaining method for gel electrophoresis of BSA demonstrate that the protein can be directly observed by naked eyes at as low as 2 ng level under a normal UV fluorescence electrophorogram gel image system.

Introduction

Over the past 20 years, boradiazaindacenes (difluoro-boradipyrromethenes, boron-dipyrromethene, BODIPYs or BDPs) as fluorescent dyes have attracted considerable attention[1] because they present many advantageous properties, such as high molar extinction coefficients (ε), high fluorescence quantum yields (Φ_f), and narrow spectra in absorption and emission at visible light.[2a] Furthermore, they are amenable to structural modification[1] and show extreme versatility.[2b] All of these attributes stimulate their applications in biomolecular labeling,[3] such as DNA sequencing, nucleic acid detection, protein analysis, real-time PCR, etc. In recent years, interests in BODIPY-based fluorogenic probes for cellular and in vivo imaging applications have grown as a result of their advantageous photophysical properties.[4] In most of the applications, BODIPY derivatives have been coupled covalently to biomolecules.

(1) Loudet, A.; Burgess, K. *Chem. Rev.* **2007**, *107*, 4891–4932.
(2) (a) Karolin, J.; Johansson, L. B-A.; Strandberg, L.; Ny, T. *J. Am. Chem. Soc.* **1994**, *116*, 7801–7806. (b) Ulrich, G.; Ziessel, R.; Harriman, A. *Angew. Chem., Int. Ed.* **2008**, *47*, 1184–1201.

(3) (a) Gonçalves, M. S. T. *Chem. Rev.* **2009**, *109*, 190–212. (b) Meng, Q. L.; Kim, D. H.; Bai, X. P.; Bi, L. R.; Turro, N. J.; Ju, J. Y. *J. Org. Chem.* **2006**, *71*, 3248–3252. (c) Aharoni, A.; Weiner, L.; Lewis, A.; Ottolenghi, M.; Sheves, M. *J. Am. Chem. Soc.* **2001**, *123*, 6612–6616. (d) Nishiya, T.; Toma, C.; Worsfold, O. *Biosens. Bioelectron.* **2004**, *19*, 1505–1511. (e) Panten, U.; Wos-Maganga, M.; Zünkler, B. J. *Biochem. Pharmacol.* **2004**, *67*, 1437–1444. (f) Turnbull, J. E.; Yates, E. A.; Atrih, A.; Dumxa-Vorzet, A. F.; Guimond, S. E.; Skidmore, M. A. *J. Chromatogr. A* **2006**, *1135*, 52–56. (g) Yee, M. C.; Fas, S. C.; Stohlmeyer, M. M.; Wandless, T. J.; Cimprich, K. A. *J. Biol. Chem.* **2005**, *280*, 29053–29059. (h) Willard, F. S.; Kimple, A. J.; Johnston, C. A.; Siderovski, D. P. *Ana. Biochem.* **2005**, *340*, 341–351. (i) Jang, H. G.; Park, M.; Wishinok, J. S.; Tannenbaum, S. R.; Wogan, G. N. *Anal. Biochem.* **2006**, *359*, 151–160. (j) Horn, T.; Chang, C.; Urdea, M. S. *Nucleic Acids Res.* **1997**, *25*, 4842–4849. (k) Lavis, L. D.; Raines, R. T. *ACS Chem. Biol.* **2008**, *3*, 142–155. (l) Peters, I. R.; Helps, C. R.; Hall, E. J.; Day, M. J. *J. Immunol. Methods* **2004**, *286*, 203–217.

DOI: 10.1021/jo901149y Published on Web 09/22/2009

SCHEME 1[a]

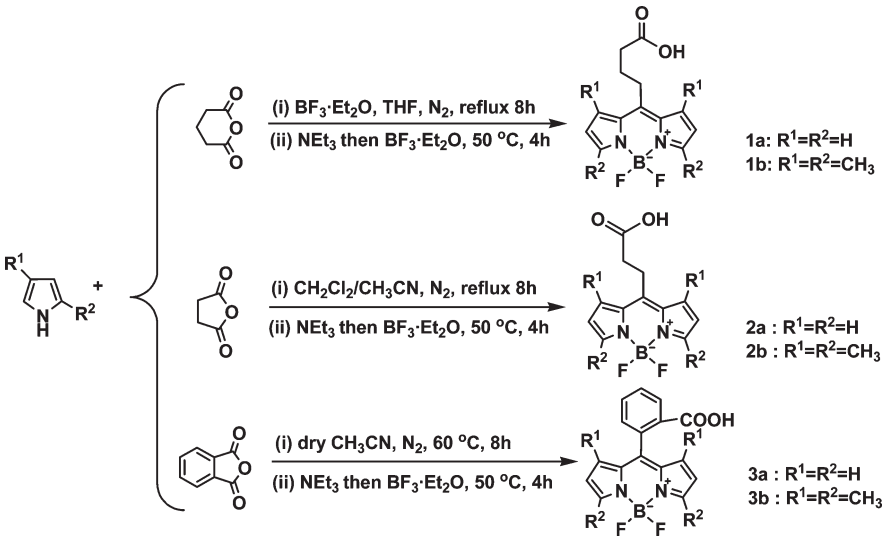

[a]Reagents and conditions. **1a** and **1b**: (i) 2.4 equiv of $BF_3{\cdot}OEt_2$, dry THF; (ii) 8 equiv of NEt_3 and 6 equiv of $BF_3{\cdot}OEt_2$. **2a** and **2b**: (i) dry CH_2Cl_2 and CH_3CN; (ii) 6 equiv of NEt_3 and 8 equiv of $BF_3{\cdot}OEt_2$. **3a** and **3b**: (i) dry CH_3CN; (ii) 6 equiv of NEt_3 and 8 equiv of $BF_3{\cdot}OEt_2$. Yields: **1a**, 25%; **1b**, 23%; **2a**, 23%; **2b**, 21%; **3a**, 26%; **3b**, 25%.

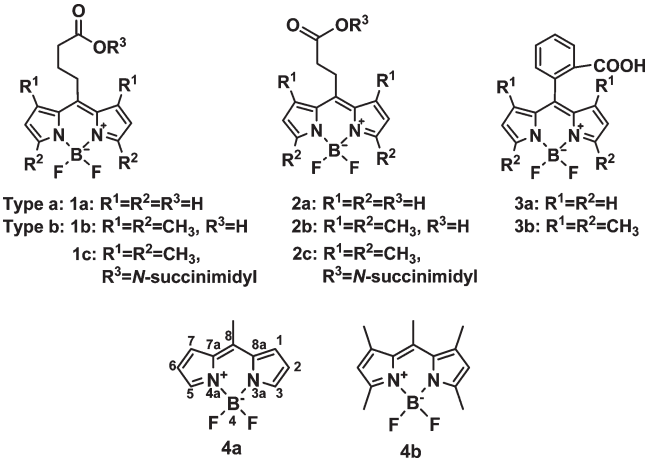

FIGURE 1. Molecular structures of BODIPY derivatives.

Although there are several ways to covalently link the dyes to biomolecules, the reaction of NHS (ester of *N*-hydroxylsuccinimidyl group) of carboxyl dyes with amino groups on target biomolecules is most useful in fluorescent labeling.[5−7] In most cases, the carboxyl group is at C-2, C-3, or C-5 positions[2,3c,f] on the skeleton of BODIPY molecules. The synthesis of the asymmetrical dyes is always from two different pyrroles, and one of them should contain a carboxyl group, which is very difficult to synthesize.[3c,g−i,6,8] For example, Alexandrova and co-workers[9] reported that an activated BODIPY-NHS ester at the C-2 position was successfully applied for DNA labeling during post-PCR target preparation for microarray analysis, where the procedure was up to seven steps and the total yield was very low (ca. 12%). So, the carboxyl BODIPY dyes with easier and more convenient synthesis procedure are significant for their practical applications.

Herein we report a simple synthesis of BODIPY dyes containing a free carboxyl group: 2 equiv of pyrrole react with 1 equiv of anhydride of dicarboxylic acid, a free carboxyl group releasing directly during the formation of the BODIPY dyes in one pot. The BODIPY dyes (Figure 1) with a carboxyl at the C-8 position show much more molecular symmetry and weaker polarity. As photodegradation mediated by photochemical oxidation is an inherent deficiency of the BODIPY dyes,[10] the structure−photostability relationship in different solvents is also investigated. Two lightfast dyes (**1a** and **2a**) are revealed and used in BSA labeling for protein gel electrophoresis (SDS−PAGE) via NHS esters of the dyes.

Results and Discussion

Synthesis. The new dyes containing different free carboxyl groups (2-carboxylethyl, 3-carboxylpropyl, and 2-caboxylphenyl) were prepared by a facile one-pot synthesis. Although a similar synthesis method was mentioned by Li et al.,[11] we improved the synthesis and separation steps. The reaction route is presented in Scheme 1: dipyrrolemethenes are prepared by the condensation of dicarboxylic anhydrides and pyrroles, which further form the new dyes by the coordination

(4) (a) Ueno, T.; Urano, Y.; Kojima, H.; Nagano, T. *J. Am. Chem. Soc.* **2006**, *128*, 10640–10641. (b) Rose Tyler, M.; Prestwich Glenn, D. *ACS Chem. Biol.* **2006**, *1*, 83–92. (c) Gabe, Y.; Urano, Y.; Kikuchi, K.; Kojima, H.; Nagano, T. *J. Am. Chem. Soc.* **2004**, *126*, 3357–3367.

(5) Hermanson, G. T. *Bioconjugate Techniques*, 2nd ed.; Thermo Fisher Scientific: Rockford, IL, 2008.

(6) Farber, S. A.; Pack, M.; Ho, S.-Y.; Johnson, I. D.; Wagner, D. S.; Dosch, R.; Mullins, M. C.; Hendrickson, H. S.; Hendrickson, E. K.; Halpern, M. E. *Science* **2001**, *292*, 1385–1388.

(7) Palomo, J. M.; Lumbierres, M.; Waldmann, H. *Angew. Chem., Int. Ed.* **2006**, *45*, 477–481.

(8) Meltola, N. J.; Wahlroos, R.; Soini, A. E. *J. Fluoresc.* **2004**, *14*, 635–647.

(9) Alexandrova, L. A.; Jasko, M. V.; Belobirtskaya, E. E.; Chudinov, A. V.; Mityaeva, O. N.; Naasedkina, T. V.; Zasedatelev, A. S.; Kukhanova, M. K. *Bioconjugate Chem.* **2007**, *18*, 886–893.

(10) Jones, G. II; Klueva, O.; Kumar, S.; Pacheco, D. *Solid State Lasers SPIE* **2001**, *24*, 4267–4271.

(11) Li, Z.; Mintzer, E.; Bittman, R. *J. Org. Chem.* **2006**, *71*, 1718–1721.

SCHEME 2. Synthesis Route of 1c

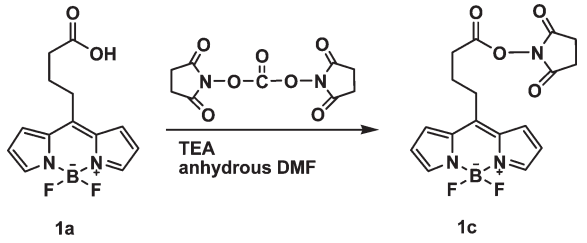

SCHEME 3. Synthesis route of 2c

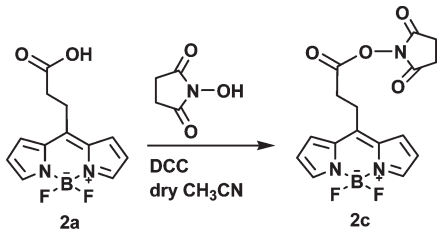

of $BF_3 \cdot OEt_2$. The key step to influence the total yield of the preparation is the first step. Anhydrous or dry conditions are important for the reaction, so molecular sieves (4 Å) should be applied to get rid of the resultant water during the reaction. Considering that the dicarboxylic anhydrides are not so soluble in CH_2Cl_2, by choosing a suitable solvent such as dry THF for dye **1a**, the yields are up to 25% after column purification.

Although the synthesis of the carboxyl BODIPY dyes can be from the reaction of pyrroles with appropriate aldehydes,[12] acyl halides[13] and free acids,[9] the procedures are too long, and the total yields are much less than 25%. So the present reaction from dicarboxylic anhydrides should be more convenient as it is a one-pot process and can release a free carboxyl group directly during the formation of the BODIPY framework.

The esters of dyes by NHS (*N*-hydroxysuccinimide) are obtained via *N*,*N*′-disuccinimidyl carbonate (dye **1c**, Scheme 2) or *N*-hydroxysuccinimide/dicyclohexylcarbodiimide (dye **2c**, Scheme 3). The reactions are mild, and the yields are above 90%. The purification should be carried out as quickly as possible by silica gel column chromatography with dry eluent at low temperature. We were very fortunate to purify and verify the activated dye-NHS ester derivatives by NMR and single crystal X-ray (for **2c**). To the best of our knowledge, this is the first report on the single crystal X-ray of an activated dye-NHS ester.

X-ray Structures of Dyes 3a and 2c. Compound **3a** and **2c** are crystallized in the monoclinic space group *P*2(1)*c*, and the triclinic space group *P*-1 respectively (Figures 2 and 3). The

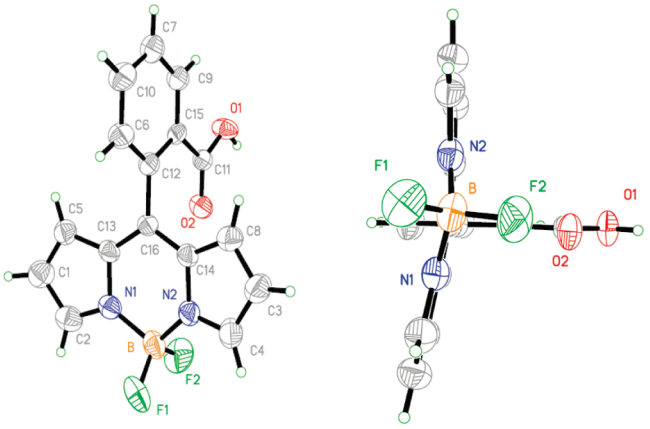

FIGURE 2. ORTEP views of the molecular structures of **3a** with thermal ellipsoids shown at 40%. All hydrogen atoms and partial carbons have been omitted for clarity.

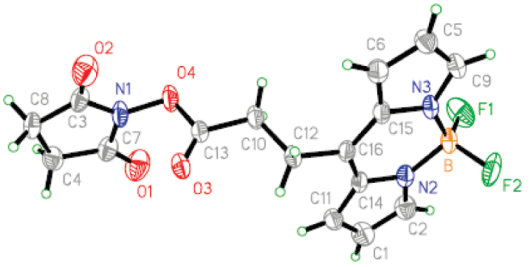

FIGURE 3. ORTEP view of the molecular structure of **2c** with thermal ellipsoids shown at 40%. All hydrogen atoms have been omitted for clarity.

BODIPY skeletons formed by three conjugated heterocyclic rings (the central six-membered ring with two adjacent five-membered rings) of the two compounds are almost planar, with the root-mean-square (rms) deviation from the least-squares mean plane for the 12 atoms of 0.109(3) and 0.032(2) Å, respectively, indicating strong π-electron delocalization within the two main planes. The average B−N distances of **3a** and **2c** are 1.539(4) and 1.540(4) Å, respectively, implying the usual delocalization of the positive charge. As for compound **3a**, probably due to steric repulsion from the hydrogen atoms of C5 and C8 and *o*-carboxyl at C15, the carboxyphenyl ring plane is strongly twisted out of the BODIPY main plane, with a dihedral angle of 84.8(2)°.

The crystal packing of **3a** and **2c** are given in Figures 10b and 4, respectively. All molecules are nearly parallel to each other with head-to-tail orientation. The carboxyphenyl ring plane of **3a** is almost orthogonal to the BODIPY main plane of the other molecules, and therefore no $\pi-\pi$ stacking interactions can be observed. Interestingly, a number of C−H···F and C=O···H intermolecular hydrogen bonds in compound **2c** and C=O···H interactions in compound **3a** help to establish the crystal packing.

Photophysical Properties. The typical absorption and fluorescence emission spectra of the carboxyl BODIPY derivatives are shown in Figures 5 and 6. The absorbance and fluorescence properties and the relative quantum yields of fluorescence (Φ_f) in various solvents are summarized in Table 1. The absorption and emission spectral maxima of the dyes are at 495 ± 10 and 510 ± 10 nm, respectively, which are

(12) (a) Laurent, P.; Olivier, M.; Mireille, B. D. *Tetrahedron Lett.* **2006**, *47*, 1913–1917. (b) Sunahara, H.; Urano, Y.; KoJima, H.; Nagano, T. *J. Am. Chem. Soc.* **2007**, *129*, 5597–5604. (c) DiCesare, N.; Lakowicz, J. R. *Tetrahedron Lett.* **2001**, *42*, 9105–9108. (d) Zrig, S.; Rémy, P.; Andrioletti, B.; Rose, E.; Asselberghs, I.; Clays, K. *J. Org. Chem.* **2008**, *73*, 1563–1566. (e) Peter, C.; Billich, A.; Ghobrial, M.; Högenauer, K.; Ullrich, T.; Nussbaumer, P. *J. Org. Chem.* **2007**, *72*, 1842–1845.

(13) (a) Chen, J.; Burghar, A.; Wan, C. W.; Thai, L; Ortiz, C.; Reibenspies, J.; Burgess, K. *Tetrahedron Lett.* **2000**, *41*, 2303–2307. (b) Wada, M.; Ito, S.; Uno, H.; Murashima, T.; Ono, N.; Urano, T.; Uranod, Y. *Tetrahedron Lett.* **2001**, *42*, 6711–6713. (c) Tahtaoui, C.; Thomas, C.; Rohmer, F.; Klotz, P.; Duportail, G.; Mély, Y.; Bonnet, D.; Hibert, M. *J. Org. Chem.* **2007**, *72*, 269–272. (d) Ulrich, G.; Ziessel, R. *J. Org. Chem.* **2004**, *69*, 2070–2083.

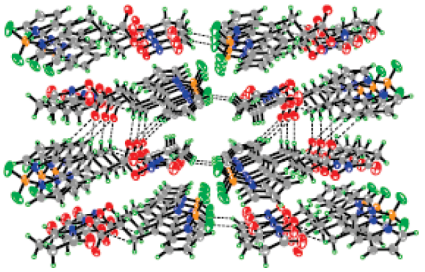

FIGURE 4. Crystal packing of **2c**. Hydrogen bonds have been indicated with thin dashed lines for clarity.

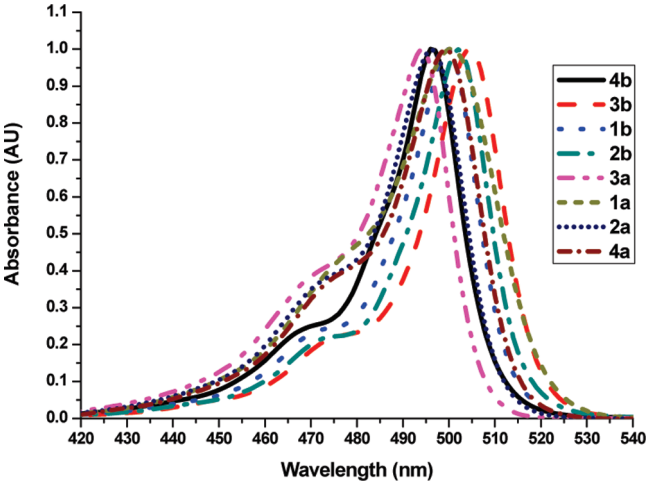

FIGURE 5. Normalized absorption spectra of dyes (ca. 1×10^{-5} M) in dichloromethane.

typical characteristics of BODIPY dyes. With the solvent polarity increases, the carboxyl BODIPY derivatives show little hypsochromic shift (e.g., for **3a**, $\lambda_{max,abs}$ 499 nm in hexane and 496 nm in water; for **1b**, $\lambda_{max,em}$ 510 nm in hexane and 505 nm in water), which indicates that the ground-state dipole moments of dyes are small.[14] The insensitivity to the polarity of solvents is very important for bioanalyzing, for the dye labeled on a biomolecule should emit stable fluorescence and be independent of various external environments. On the other hand, type **b** (**1b**, **2b**, and **3b** with four methyl groups) display molar extinction coefficients much larger than those of type **a** (**1a**, **2a** and **3a** without methyl group), which is probably the result of electronic effect of the methyl groups.[15]

As we know, high fluorescence quantum yields are very important for the applications of fluorescent dyes, especially in aqueous media. For the conjugation reactions involving biologically relevant macromolecules must be performed in water or aqueous buffers. Table 1 shows that the new BODIPY dyes have excellent fluorescence quantum yields even in water (up to 0.80 for **1b**), of which type **b** are relatively higher than those of type **a**. In organic solvent, such as dichloromethane, the values of **1a** and **2a** are 0.65 and 0.67, respectively, whereas the related values of **1b** and **2b** are 0.85 and 0.83, respectively. This difference between the

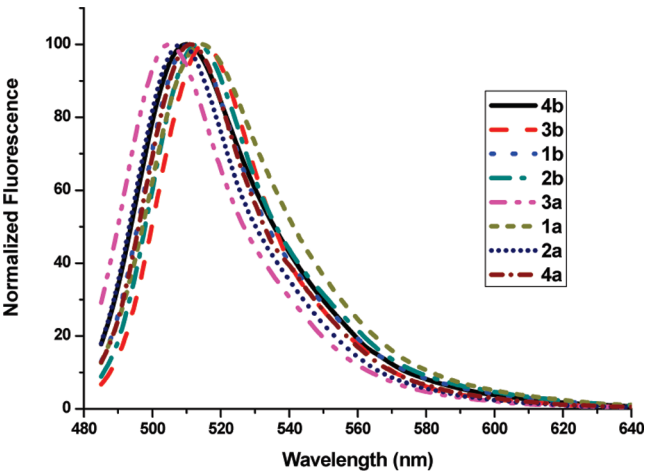

FIGURE 6. Normalized fluorescence emission spectra of dyes (ca. 2×10^{-6} M) in dichloromethane.

two kinds of dyes might be due to their different electronic effects: the electron-donating effect of the methyl groups on the BODIPY skeleton should play a great role in their relative quantum yields of fluorescence.[16]

For the difference of **3a** and **3b**, the steric effect is another factor to influence fluorescence quantum yield. From the X-ray structure of **3a** (Figure 2), the steric interaction between 2-carboxyphenyl at C-16 and the two hydrogen atoms at C-8 and C-5 on BODIPY make the phenyl plane nearly perpendicular to the BODIPY plane, with the dihedral angle of 84.8(2)°. Dye **3b**, with two bulky methyl groups at C-1 and C-7 positions (Figure 1), should behave more steric effect than **3a**. The steric effects can suppress the efficiency of internal conversion (IC) via intramolecular vibronic relaxation and result in larger fluorescence quantum yields.[17]

Photostability. High photostability of fluorescence dyes is one of the most important characters for practical applications.[13] To track the photofading of the new dyes, their solutions were irradiated with a 500 W *I-W* lamp to test the photostability to irradiation (see Supporting Information for details). A decrease of their maximal absorption both in deaerated acetonitrile and in aerated water with different irradiation times was detected and is illustrated in Figures 7 and 8, respectively. As shown in Figure 7, the photostability of **3b** and **3a** with 2-carboxyphenyl at C-8 position are relatively lower than those with carboxyalkyl groups, **2b** (or **1b**) and **2a** (or **1a**).

The four methyl groups in type **b** increased the electron cloud density of dye molecules and made them easier to be oxidized and less photostable than type **a**. This also explained a greater contribution of the electronic factor in BODIPY skeleton for the dyes both with rigid phenyl and flexible alkyl carboxyl groups at C-8. The phenomenon is drastically evident by their comparison in aerated water as illustrated in Figure 8. After irradiation for 1 h, the

(14) Rurack, K.; Kollmansberger, M.; Daub, J. *Angew. Chem., Int. Ed.* **2001**, *40*, 385–387.
(15) Qin, W. W.; Baruah, M.; Auweraer, M. V.; Schryver, F. C. D.; Boens, N. *J. Phys. Chem. A* **2005**, *109*, 7371–7384.
(16) (a) Herradón, B.; Chana, A.; Alonso, M.; Liras, M. *J. Mol. Struct.* **2004**, *697*, 29–40. (b) Haefele, A.; Ulrich, G.; Retailleau, P.; Ziessel, R. *Tethrhedron Lett.* **2008**, *49*, 3716–3721. (c) Goze, C.; Ulrich, G.; Mallon, L. J.; Allen, B. D.; Harriman, A.; Ziessel, R. *J. Am. Chem. Soc.* **2006**, *128*, 10231–10239.
(17) Li, F.; Yang, S. I.; Lindsey, J. S. *J. Am. Chem. Soc.* **1998**, *120*, 10001–10017.

TABLE 1. Photophysical Properties of the Dyes in Different Solvents[a]

dye	solvent	λ_{max} (abs, nm)	$\lambda_{max}{}^{b}$ (em, nm)	$\triangle\lambda^{c}$ (nm)	E^{d} 10^5 (M^{-1} cm^{-1})	$\Phi_f{}^{e}$
1a	hexane	496	508	12	0.55	0.63
	DCM[f]	496	508	12	0.50	0.65
	ethanol	492	503	11	0.52	0.62
	H_2O[g]	490	502	12	0.46	0.60
1b	hexane	500	510	10	0.79	0.76
	DCM	500	511	11	0.80	0.85
	ethanol	496	506	10	0.81	0.82
	H_2O	493	505	12	0.73	0.80
2a	hexane	498	509	11	0.53	0.62
	DCM	499	511	12	0.54	0.67
	ethanol	492	505	13	0.56	0.66
	H_2O	492	504	12	0.49	0.67
2b	hexane	502	511	9	0.81	0.77
	DCM	502	514	12	0.80	0.83
	ethanol	496	505	9	0.83	0.79
	H_2O	494	506	12	0.82	0.78
3a	hexane	499	514	15	0.56	0.55
	DCM	501	515	14	0.57	0.64
	ethanol	496	513	17	0.55	0.60
	H_2O	496	514	17	0.52	0.58
3b	hexane	503	514	11	0.82	0.70
	DCM	505	515	10	0.83	0.73
	ethanol	500	510	10	0.81	0.71
	H_2O	497	510	13	0.80	0.72
4a	hexane	496	504	8	0.68	0.70
	DCM	494	505	11	0.68	0.73
	ethanol	490	502	12	0.66	0.71
4b	hexane	498	509	11	1.07	0.85
	DCM	496	510	14	0.89	0.92
	ethanol	494	507	13	0.96	0.88

[a]All Φ_f values are corrected for changes in refractive indexes of different solvents used. No data listed on the optical properties of **4a** and **4b** in water for the insolubility. [b]Emission spectra were measured with different excitation wavelengths: λ_{ex} = 485 nm for type **a** and **4a**; λ_{ex} = 490 nm for type **b** and **4b**. [c]Stokes shift. [d]Molar extinction coefficients are in the maximum of the highest peak. [e]Fluorescence quantum efficiency was determined using that of fluorescein (Φ_f = 0.85 in 0.1N NaOH) as a standard. [f]Dichloromethane. [g]DD water.

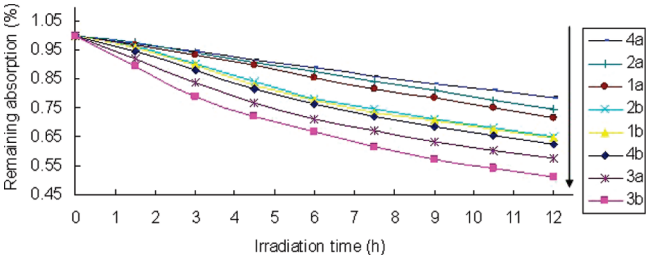

FIGURE 7. Comparisons on the photofading of the dyes (ca. 1 × 10^{-5} M) in deaerated acetonitrile.

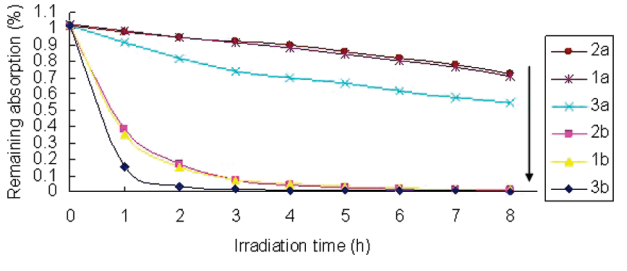

FIGURE 8. Comparisons on the photofading of the dyes (ca. 1 × 10^{-5} M) in aerated water.

absorption intensity of type **b** dyes decreased sharply: the residual absorption of dye **2b** and dye **3b** is only 40% and 15%, respectively, whereas dye **2a** and dye **3a** still retained higher residual absorption (72% and 54% respectively) after 8 h.

TABLE 2. Solution Electrochemical Properties of the Dyes[a]

dyes	$E'^{0}{}_{ox}$, V ($\triangle E$, mV)	$E'^{0}{}_{red}$, V ($\triangle E$, mV)
1a	+1.27 (irrev)	−1.03 (80)
2a	+1.25 (irrev)	−1.08 (70)
3a	+1.06 (irrev); +1.40 (irrev)	−1.10 (60)
4a	+1.29 (irrev)	−1.01 (70)
1b	+1.06 (70)	−1.41 (80)
2b	+1.05 (70)	−1.39 (80)
3b	+0.96 (80); +1.26 (irrev)	−1.50 (70)
4b	+1.07 (60)	−1.32 (60)

[a]Potentials determined by cyclic voltammetry in deoxygenated CH_3CN solutions, containing 0.1 M $TBAPF_6$, at a solute concentration of 1−6 × 10^{-3} M, at rt. Potentials were standardized with ferrocene (Fc) as internal reference assuming that $E_{1/2}$ (Fc/Fc^+) = +0.43 V ($\triangle E_p$ = 70 mV) vs $Ag/AgNO_3$. Error in half-wave potentials is ±10 mV. Scan rate 100 mV/s. When the redox process is irreversible, the peak potentials (E_{ap}) are quoted.

The electrochemical properties of the dyes were investigated by cyclic voltammetry in acetonitrile. The data shown in Table 2 demonstrate that oxidation potentials of type **b** are much lower than those of type **a**, for example, the values of **1a** and **1b** are 1.27 and 1.06 V, respectively, which clearly shows that **1a** is more resistant to oxidization than **1b**.

Mackey and co-workers reported[18] that the photodegradation of BODIPY dyes is mediated by a singlet oxygen ($^1O_2$) photooxidation mechanism. Mula and co-workers[19] also pointed out that the photostability of BODIPY dyes is dependent on their capacities to generate $^1O_2$ and probability

(18) Mackey, M. S.; Sisk, W. N. *Dyes Pigments* **2001**, *51*, 79–85.
(19) Mula, S.; Ray, A. K.; Banerjee, M.; Chaudhuri, T.; Dasgupta, K.; Chattopadhyay, S. *J. Org. Chem.* **2008**, *73*, 2146–2154.

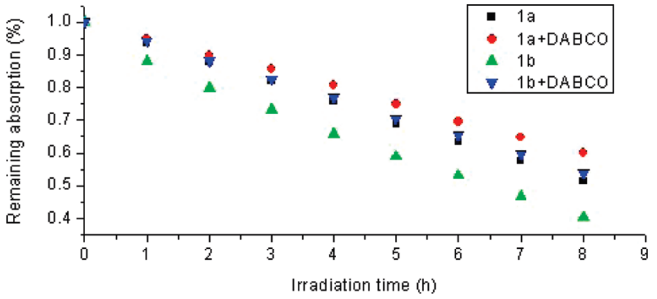

FIGURE 9. Effect of DABCO on the photofading of dyes **1a** and **1b** (ca. 1×10^{-5}M) in aerated water.

of reaction with $^1O_2$. In the present cases, a $^1O_2$ quencher, 1,4-diazabicyclo[2,2,2]octane (DABCO), had the effect to improve the photostability of the dye solutions (Figure 9) to some extent. So, $^1O_2$ is proved to be one of the main factors to the photodecomposition.

On the other hand, the effect of different solvents should be considered for the different probability of producing $^1O_2$ and lifetime of $^1O_2$.[20] In general, the dyes with less π electron cloud density probably have higher photostability in polar protic and aprotic solvents, and the influence of the electronic effect is remarkable especially in water.

Furthermore, from the molecular packing in the crystal structure of **4a** and **3a** as schematically indicated in Figure 10, the most striking feature is the totally different form of the intermolecular hydrogen bond. Generally, the BF_2 acts as a functional group in the BODIPY molecule, of which the F atom shows strong electronegativity and probably forms a hydrogen bond. This was proved by the X-ray structure of **4a** (B−F···H−C hydrogen bonds in Figure 10a), but it is not the case as for **3a** (only C═O···H−O hydrogen bonds in Figure 10b). Since the final cleavage of N−B bond in the BODIPY core arise from the photofading or photooxydation,[10,19] the existence of the B−F···H−C hydrogen bonds in BODIPY molecules will strengthen the process of the excited-state deactivation by a nonradiative transition[21] and further decrease the probability of reaction with $^1O_2$ to a great extent. The 2-carboxyphenyl at C-8 in **3a** changed the normal arrangement of single crystal structure, which destroyed the intermolecular hydrogen bond (B−F···H−C) in the BODIPY main skeleton. In this case, the excited state of **3a** becomes unstable and can be more easily attacked by $^1O_2$. The experimental results also rationalized the assumption.

To prove the effect of hydrogen bonds in solution on the photostability of the dye molecules, ^{1}H NMR experiments with dyes **3a** and **4a** were further carried out in both $CDCl_3$ and CD_3OD. The results (Figure S24 in Supporting Information) show that the protons of methyl and pyrrole rings in **4a** (and **3a**) shift to lower magnetic field when the solvent is changed from aprotic $CDCl_3$ to protic CD_3OD. This means that there are intermolecular hydrogen bonds between dye molecules in aprotic solution. In a protic solution such as methanol or water, these bonds are very weak or disappear. This might be one of the reasons why the photostability in water is much lower.

BSA Labeling and Electrophoresis Analysis. Considering excellent photostability and reasonable spectral properties of dyes **1a** and **2a**, we chose both of them to investigate the optimum labeling conditions and their detection limits (LOD) for protein labeling after activation by esterification. Herein, only the labeling results of activated dye **1c** with BSA are illustrated (Figure 11). The pH of the buffer solution is critical for the protein labeling reaction. As shown in Figure 11a, in the range of pH 8.0−9.5, pH 9.0 was the optimum for the best labeling intensity. Moreover, we investigated the effect of different molar ratio of BSA/dye. Both lane 3 and lane 4 in Figure 11b show bright labeled spots, whereas the others are not so strong. The spots on the bottom of lane 4 and lane 5 show that the dye **1c** is superfluous for BSA labeling, so molar ratio 1/20 (BSA/dye) is chosen as optimum ratio.

In fact, numerous methods are commercially available that enable fluorescent stain and detection of proteins in SDS−PAGE gels. SYPRO Red, for example, is one of most popular fluorescent poststains by binding noncovalently and unspecifically to the SDS-coat surronunding the proteins, which has LODs as low as 1−2 ng of protein.[22] In comparison to the popular and well-established technique of tedious and troublesome poststaining, the prestaining is simple, clean, time-saving, environment-friendly, and very sensitive.[23] Since the LODs somewhat depend on the staining conditions and imaging systems, in our study, **1c** is a BODIPY-based prelabel that covalently bind to protein, and the LOD (Figure 11c) is as low as 2 ng (ca. 6 nM) under optimized incubation conditions: molar ratio of BSA/dye 1:20, reaction at 30 °C for 40 min at pH 9.0. So, BODIPY dyes, as a new kind of fluorogenic amino-reactive prestain label that covalently binds to the proteins, show great value for potential applications.

Conclusions

In summary, an important strategy for the synthesis of BODIPY dyes with a carboxyl group from pyrroles and dicarboxylic anhydrides in one-pot reactions has been developed, which is much more convenient and efficient than most common methods reported before. The methyl groups on the BODIPY ring had a positive influence on the fluorescence quantum yields (Φ_f) but a negative effect on the photostability. Several factors including electronic effect, steric restriction, and intermolecular hydrogen bonding, as well as solvent effect, were analyzed and investigated for photooxidation bleaching reaction, which proved the synergy effect and clarified the experimental observations rationally. BSA labeling experiments show that the activated dyes **1c** and **2c** with a free carboxyalkyl group at C-8 are suitable for bioanalyzing in terms of their excellent photostability, easy synthesis, and high sensitivity. The study should provide convenient and wide usage of BODIPY derivatives with carboxyl in bioanalysis and biolabeling.

Experimental Section

General Procedure A for the Synthesis of BODIPY Derivatives with Carboxyl. To a solution of 1.67 equiv of 2,4-dimethylpyrrole (or pyrrole) in suitable solvent was added 1 equiv of

(20) Rodgers, M. A. J. *J. Am. Chem. Soc.* **1983**, *105*, 6201–6205.
(21) Sobolewski, A. L.; Domcke, W.; Httig, C. *J. Phys. Chem. A* **2006**, *110*, 6301–6306.
(22) Berggren, K.; Chernokalskaya, E.; Steinberg, T.; Kemper, C.; Lopez, M.; Diwu, Z.; Haugland, R.; Patton, W. *Electrophoresis* **2000**, *21*, 2509–2521.
(23) (a) Barger, B.; White, F.; Pace, J.; Kemper, D.; Ragland, W. *Anal. Biochem.* **1976**, *70*, 327–335. (b) Tonge, R.; Shaw, J.; Middleton, B.; Rowlinson, R.; Young, S.; Pognan, F.; Hawkins, E.; Currie, I.; Davison, M. *Proteomics* **2001**, *1*, 377–396. (c) Shaw, J.; Rowlinson, R.; Nickson, J.; Stone, T.; Sweet, A.; Williams, K.; Tonge, R. *Proteomics* **2003**, *3*, 1181–1195.

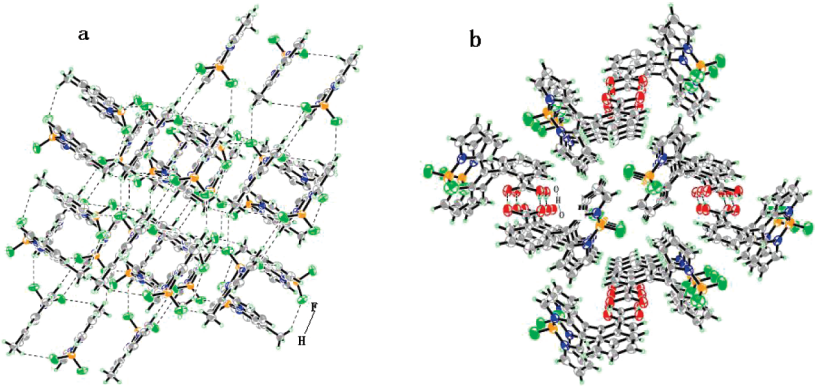

FIGURE 10. Crystal packing of **4a** (a) and **3a** (b). Hydrogen bonds have been indicated with thin dashed lines for clarity.

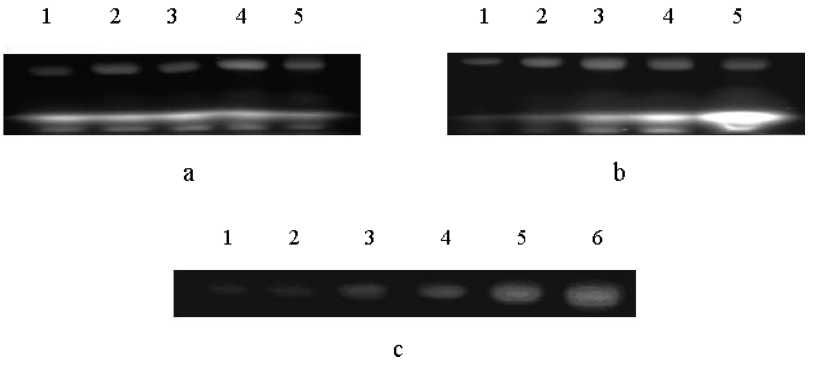

FIGURE 11. Fluorescence image of BSA labeled with **1c** after electrophoresis. Labeling conditions: (a) BSA/**1c** = 1/10 (molar ratio); BSA = 5 μg; reaction temperature = 30 °C; pH for lane 1 = 8.0, lane 2 = 8.4, lane 3 = 8.7, lane 4 = 9.0, lane 5 = 9.5. (b) BSA = 5 μg; pH = 9.0; reaction temperature = 30 °C; BSA/**1c** for lane 1 = 1/5, lane 2 = 1/10, lane 3 = 1/20, lane 4 = 1/40, lane 5, 1/100. (c) **1c** = 3.6×10^{-9} mol (1 μg/μL in acetonitrile); buffer = pH 9.0; reaction temperature = 30 °C; time = 40 min; BSA for lane 1 = 2 ng, lane 2 = 5 ng, lane 3 = 10 ng, lane 4 = 20 ng, lane 5 = 50 ng, lane 6 = 200 ng.

anhydride. The solution was stirred at a certain temperature for 8 h; 2 equiv of boron trifluoride etherate may be added into the solution before the reaction. Triethylamine (6.7 equiv) was then added, followed by a subsequent addition of boron trifluoride etherate (6.7 equiv). The mixture was stirred for 4 h at 50 °C and then was washed three times with water. The organic layer was dried over Na_2SO_4 or $MgSO_4$ and filtered, and the solvent was removed. Chromatography on silica gel gave the pure compounds.

4-(4,4-Difluoro-1,3,5,7-tetramethyl-4-bora-3a,4a-diaza-*s*-indacene-8-yl)-butyric Acid 1b. To a two-necked flask were added sequentially glutaric anhydride (204 mg, 1.8 mmol), dry THF (30 mL), 2,4-dimethylpyrrole (280 mg, 3 mmol), and $BF_3 \cdot OEt_2$ (0.51 g, 3.6 mmol). The mixture was heated to reflux for 8 h under nitrogen. After the mixture was cooled to room temperature, Et_3N (1.21 g, 12 mmol) and then $BF_3 \cdot OEt_2$ (1.28 g, 9 mmol) were added slowly, respectively. The reaction mixture was stirred at 50 °C for 4 h, washed with water (3 × 15 mL), and extracted with CH_2Cl_2 (3 × 100 mL). The organic fraction was dried over anhydrous Na_2SO_4, and the solvent was removed. The residue was purified by silica gel (hexane/EtOAc/HOAc, 80:40:1) and gave 115 mg of dye **1b**. Brick red needle. Yield: 23%. Mp: 152−153 °C. HRMS (TOF MS EI^+) calculated for $C_{17}H_{21}BF_2N_2O_2$ 334.1664, found 334.1657. ^{1}H NMR ($CDCl_3$, 400 MHz) δ 6.07 (s, 2H, pyrrole-H), 3.32 (t, 2H, -CH_2, J = 8.8 Hz), 2.64 (t, 2H, -CH_2, J = 8.8 Hz), 2.52 (s, 6H, -CH_3), 2.44 (s, 6H, -CH_3), 1.32 (t, 2H, -CH_2); ^{13}C NMR ($CDCl_3$, 100 MHz) δ 176.9, 154.9, 143.3, 140.6, 131.4, 122.2, 35.6, 23.7, 16.6, 14.7.

3-(4,4-Difluoro-1,3,5,7-tetramethyl-4-bora-3a,4a-diaza-*s*-indacene-8-yl)-propionic Acid 2b. In a round-bottom flask, a mixture of succinic anhydride (200 mg, 2.0 mmol) and 2,4-dimethylpyrrole (457 mg, 4.80 mmol) dissolved in a mixture of dry CH_2Cl_2 (20 mL) and dry CH_3CN (5 mL) was heated to reflux under N_2 for 8 h. After the solution was cooled to room temperature, 6 equiv of Et_3N (1.21 g, 12 mmol) was added slowly, and after a while, 8 equiv of $BF_3 \cdot OEt_2$ (2.27 g, 16 mmol) was added continuously. The reaction mixture was strongly stirred under N_2 at 50 °C for another 4 h. The mixture was quenched and washed with water (3 × 15 mL) and extracted with CH_2Cl_2 (3 × 100 mL), and then the organic phase was washed with brine and dried over anhydrous $MgSO_4$. Finally the solvent was evaporated in vacuum. Column chromatography on silica gel (CH_2Cl_2/EtOAc, gradient from 4:1 to 1:1) afforded 134 mg of the title compound as an orange red powder. Yield: 21%. Mp: 173−174 °C. HRMS (TOF MS ES^-) calculated for $C_{16}H_{19}BF_2N_2O_2$ 319.1429, found 319.1435. ^{1}H NMR ($CDCl_3$, 400 MHz) δ 6.08 (s, 2H, pyrrole-H), 3.34 (t, 2H, -CH_2, J = 8.8 Hz), 2.67 (t, 2H, -CH_2, J = 8.8 Hz), 2.85 (s, 6H, -CH_3), 2.53 (s, 6H, -CH_3). ^{13}C NMR ($CDCl_3$, 100 MHz) δ 176.4, 155.5, 142.8, 140.7, 131.4, 122.2, 35.1, 23.5, 16.6, 14.7.

2-(4,4-Difluoro-1,3,5,7-tetramethyl-4-bora-3a,4a-diaza-*s*-indacene-8-yl)-benzoic Acid 3b. *o*-Phthalic anhydride (296 mg, 2 mmol) and 2,4-dimethylpyrrole (380 mg, 4 mmol) were dissolved in 20 mL of dry acetonitrile, which was bubbled for 15 min in a nitrogen atmosphere and then added to a two-necked flask equipped with a magnetic stirrer, a reflux condenser, and a nitrogen input tube. After the mixture stirred at 60 °C in an oil bath under nitrogen overnight, the solution was cooled to room temperature, and 6 equiv of Et_3N (1.21 g, 12 mmol), followed by 8 equiv of $BF_3 \cdot OEt_2$ (2.27 g, 16 mmol), was injected slowly into

the solution respectively. After a while, a bright green fluorescence appeared. The mixture was stirred under a nitrogen atmosphere for another 4 h at 50 °C. Finally, the reaction mixture was washed with water three times (3 × 15 mL), extracted with CH_2Cl_2 (3 × 100 mL), dried over $MgSO_4$, filtered, and evaporated to dryness. The crude compound was subjected to flash column chromatography over silica gel (hexane/EtOAc/MeOH, 100:30:3) and afforded a red solid (177 mg, 25%). The obtained product was recrystallized from CH_2Cl_2 and hexane twice and then was used for the configuration determination. Mp: 235−237 °C. HRMS (TOF MS EI$^+$) calculated for $C_{20}H_{19}BF_2O_2N_2$ 368.1508, found 368.1504. ^{1}H NMR (CD_3COCD_3, 400 MHz) δ 11.47 (s, 1H, COOH), 8.14 (dd, J = 8.0 Hz, 1H), 7.79 (dd, ^3J = 7.6 Hz, ^4J = 1.2 Hz, 1H), 7.69 (dd, ^3J = 7.6 Hz, ^4J = 1.2 Hz, 1H), 7.42 (dd, J = 7.6 Hz, 1H), 6.03 (s, 2H), 2.45 (s, 6H, CH_3), 1.33 (s, 6H, CH_3). ^{13}C NMR (CD_3COCD_3, 100 MHz) δ 166.4, 154.6, 142.9, 142.2, 136.0, 133.4, 131.4, 131.2, 131.0, 129.9, 129.8, 121.0, 13.9, 13.5.

4-(4,4-Difluoro-4-bora-3a,4a-diaza-*s*-indacene-8-yl)-butyric Acid 1a. A procedure very similar to the synthesis of compound **1b** was applied in the synthesis of the dye **1a**. Dark red floccule. Yield: 25%. Mp: 136−137 °C. HRMS (TOF MS EI$^+$) calculated for $C_{13}H_{13}BF_2N_2O_2$ 278.1038, found 278.1031. ^{1}H NMR (CD_3CO-CD_3, 400 MHz) δ 10.73 (s, 1H, -COOH), 7.88 (s, 2H, pyrrole-H), 7.63 (d, 2H, pyrrole-H, J = 3.6 Hz), 6.61 (d, 2H, pyrrole-H, J = 4.0 Hz), 3.16 (t, 2H, -CH_2, J = 8.4 Hz), 2.51 (t, 2H, -CH_2, J = 7.6 Hz), 2.08−2.00 (m 2H, -CH_2). ^{13}C NMR (CD_3COCD_3, 100 MHz) δ 173.5, 151.2, 143.8, 135.4, 128.8, 118.3, 32.8, 29.8, 29.1.

3-(4,4-Difluoro-4-bora-3a,4a-diaza-*s*-indacene-8-yl)-propionic Acid 2a. The procedure is similar with that of dye **2b**. Dark red powder. Yield: 23%. Mp: 142−144 °C. HRMS (TOF MS EI$^+$) calculated for $C_{12}H_{11}BF_2N_2O_2$ 264.0882, found 264.0871. ^{1}H NMR ($CDCl_3$, 400 MHz) δ 7.88 (s, 2H, pyrrole-H), 7.32 (d, 2H, pyrrole-H, J = 3.6 Hz), 6.57 (d, 2H, pyrrole-H, J = 3.2 Hz), 3.28 (t, 2H, -CH_2, J = 8.0 Hz), 2.85 (t, 2H, -CH_2, J = 8.0 Hz). ^{13}C NMR ($CDCl_3$, 100 MHz) δ 177.0, 147.4, 144.5, 135.0, 128.2, 118.7, 36.7, 25.7.

2-(4,4-Difluoro-4-bora-3a,4a-diaza-*s*-indacene-8-yl)-benzoic Acid 3a. The synthesis of compound **3a** is similar with that of compound **3b**. Brick red needle. Yield: 26%. Mp: 170−172 °C. HRMS (TOF MS EI$^+$) calculated for $C_{16}H_{11}BF_2N_2O_2$ 312.0882, found 312.0886. ^{1}H NMR (CD_3COCD_3, 400 MHz) δ 11.480 (s, 1H, -COOH), 8.19 (dd, 1H, Ar-H, J = 7.6 Hz), 7.99 (s, 2H, pyrrole-H), 7.80 (t, 1H, Ar-H, J = 6.4 Hz), 7.78 (t, 1H, Ar-H, J = 6.8 Hz), 7.62 (dd, 1H, Ar-H, J = 7.6 Hz), 6.79 (d, 2H, pyrrole-H, J = 4.0 Hz), 6.59 (d, 2H, pyrrole-H, J = 4.0 Hz). ^{13}C NMR (CD_3COCD_3, 100 MHz) δ 167.1, 149.0, 144.8, 136.4, 134.9, 132.9, 132.6, 132.0, 131.5, 131.0, 130.9, 119.3. Suitable single crystals for X-ray analyses were obtained by slow evaporation of a hexane/ DCM solution.

General Procedure B for the Synthesis of BODIPY Succinimidyl Esters. To a 25 mL round-bottom flask were added 1 equiv of BODIPY derivatives with carboxyl (**1a** and **2a**) in anhydrous DMF or CH_3CN, 1.5 equiv of *N*,*N*′-disuccinimidyl carbonate (for **1a**) or 1.2 equiv of *N*-hydroxysuccinimide (for **2a**), and 7.5 equiv of triethylamine (for **1a**) or 2.5 equiv of dicyclohexylcarbodiimide (for **2a**) respectively, and the mixture was stirred under nitrogen for 12−24 h at 25 °C and monitored until total consumption of the starting material was observed by TLC. The solvent was evaporated, and the residue was dissolved in CH_2Cl_2 and washed with water twice. The organic layer was then dried over $MgSO_4$ and filtered, and the solvent was removed. A flash chromatography on silica gel and a recrystallization gave the pure compounds. All steps should be carried out at low temperature (< 25 °C).

4-(4,4-Difluoro-4-bora-3a,4a-diaza-*s*-indacene-8-yl)-butyric Acid, Succinimidyl Ester 1c. To a 25 mL round-bottom flask were added 55.6 mg of **1a** (0.2 mmol) and 77 mg of *N*,*N*′-disuccinimidyl carbonate (0.3 mmol) respectively. After 0.2 mL (1.5 mmol) of triethanolamine and 5 mL of dry DMF were injected, the mixture was stirred under nitrogen for 12−24 h at 25 °C. The whole process was monitored by TLC. After reaction, the solvent was evaporated by rotavapor under highly reduced pressure at no more than 20 °C. The residue was dissolved and extracted with CH_2Cl_2 (3 × 50 mL), washed with water (2 × 15 mL), and dried over anhydrous $MgSO_4$, and the concentrated solution was purified by flash silica column chromatography (CH_2Cl_2/EtOAc, gradient from 12:1 to 8:1). The obtained compound was recrystallized from CH_2Cl_2 and hexane and produced 67 mg of orange red powder (**1c**). Yield: 90%. HRMS (TOF MS EI$^+$) calculated for $C_{17}H_{16}BF_2N_3O_4$ 375.1199, found 375.1202. ^{1}H NMR ($CDCl_3$, 400 MHz) δ 7.87 (s, 2H, pyrrole-H), 7.365 (d, 2H, pyrrole-H, J = 4.4 Hz), 6.552 (d, 2H, pyrrole-H, J = 3.2 Hz), 3.075 (t, 2H, -CH_2, J = 8.0 Hz), 2.887 (d, 4H, -CH_2, J = 2.8 Hz), 2.783 (d, 2H, -CH_2, J = 6.4 Hz), 2.258−2.185 (m, 2H, -CH_2). ^{13}C NMR ($CDCl_3$, 100 MHz) δ 169.2, 168.1, 148.6, 144.2, 135.3, 128.3, 118.6, 30.8, 29.7, 28.3, 25.6. $\lambda_{max,abs}$ in CH_2Cl_2: 498 nm. $\lambda_{max,em}$ in CH_2Cl_2: 513 nm.

4-(4,4-Difluoro-4-bora-3a,4a-diaza-*s*-indacene-8-yl)-propionic Acid, Succinimidyl Ester 2c. To a 25 mL round-bottom flask were added 80 mg of **2a** (0.3 mmol), 42 mg of *N*-hydroxysuccinimide (0.36 mmol), and 155 mg of dicyclohexylcarbodiimide (0.75 mmol). After 8 mL of dry acetonitrile was injected, the mixture was stirred under nitrogen for about 16−24 h at 25 °C. The whole process was monitored by TLC. After reaction, the same workup procedure as for the synthesis of compound **1c** was applied and afforded 100 mg of orange red powder (**2c**). Yield: 92%. HRMS (TOF MS EI$^+$) calculated for $C_{16}H_{14}BF_2N_3O_4$ 361.1045, found 361.1013. ^{1}H NMR ($CDCl_3$, 400 MHz) δ 7.893 (s, 2H, pyrrole-H), 7.327 (d, 2H, pyrrole-H, J = 4.0 Hz), 6.583 (d, 2H, pyrrole-H, J = 3.6 Hz), 3.345 (t, 2H, -CH_2, J = 8.0 Hz), 3.069 (t, 2H, -CH_2, J = 8.0 Hz), 2.875 (s, 4H, -CH_2). ^{13}C NMR ($CDCl_3$, 100 MHz) δ 168.9, 167.1, 145.9, 144.9, 134.9, 128.2, 119.0, 33.7, 25.8, 25.6. $\lambda_{max,abs}$ in CH_2Cl_2: 502 nm. $\lambda_{max,em}$ in CH_2Cl_2: 522 nm. Suitable single crystals for X-ray analyses were obtained by slow evaporation of a $CDCl_3$ solution.

General Procedure C for the BSA Labeling with 1c. General labeling reaction procedure: 5 μg of BSA solution (1 μL) was injected in 2 μL of borax−boric acid buffer solution containing 2.5% (w/v) SDS and 1% (w/v) sucrose in an Eppendorf microtube, pH from 8.0 to 9.5, and 1 μL of dd water. After denaturalization for 4−5 min in a 100 °C water bath, a certain molar ratio of **1c** and BSA was mixed and then incubated for 30−40 min in dark at 30−50 °C.

General Procedure D for the SDS−PAGE and Gel Image. The electrophoresis experiment was carried out on a polyacrylamide mini-gel (1 mm thick) using a discontinuous buffer system. The stacking gel contained 10% polyacrylamide in a 0.4 M borax−boric acid buffer solution (pH 8.7), and the separating gel contained 5% polyacrylamide in a 0.12 M Tris-HCl buffer solution (pH 6.8). The running buffer contained 20 mM borax−boric acid, pH 8.7, 0.1% (w/v) SDS in water. All solutions were freshly prepared prior to use. SDS−PAGE was carried out on a vertical polyacrylamide gel system until the protein bands reach the interface of the separating gel. Separation was performed at a constant voltage of 105 V.

Acknowledgment. This work was supported by the National Science Foundation of China (20706008, 20705621, and 20876024), National Basic Research Program of China (2009CB724706), Ministry of Education of China (Program for Changjiang Scholars and Innovative Research Team in University, IRT0711; and Cultivation Fund of the Key Scientific and Technical Innovation Project, 707016).

Supporting Information Available: General experimental procedures (synthesis, spectroscopic measurements, photooxidation

experiments, electrochemical tests, BSA labeling with **1c**, SDS−PAGE and gel image), reagents, materials; X-ray crystallographic data of **3a** as a CIF file; X-ray crystallographic data of **2c** as a CIF file; detailed X-ray crystal structures determination and geometrical parameters for **3a** and **2c**; ^{1}H and ^{13}C NMR spectra for BODIPY derivatives (**1a**, **2a**, **3a**, **1b**, **2b** and **3b**); ^{1}H and ^{13}C NMR spectra for BODIPY succinimidyl esters (**1c** and **2c**); proton shift test (^{1}H NMR experiments) in aprotic and protic solvents at different temperature. This material is available free of charge via the Internet at http://pubs.acs.org.